

To be submitted to
Physical Review B

ISTITUTO NAZIONALE DI FISICA NUCLEARE
Laboratori Nazionali di Frascati

LNF-85/26(P)
17 Giugno 1985

M.Benfatto, C.R.Natoli, A.Bianconi, J.Garcia, A.Marcelli,
M.Fanfoni and I.Davoli: MULTIPLE SCATTERING REGIME AND
HIGHER ORDER CORRELATIONS IN X-RAY ABSORPTION SPECTRA
OF LIQUID SOLUTIONS

MULTIPLE SCATTERING REGIME AND HIGHER ORDER
CORRELATIONS IN X-RAY ABSORPTION SPECTRA OF
LIQUID SOLUTIONS

M.Benfatto,C.R.Natoli

INFN-Laboratori Nazionali di Frascati 00044 Frascati ITALY

A.Bianconi,J.Garcia*,A.Marcelli,M.Fanfoni

Dipartimento di Fisica, Universita' "La Sapienza" 00185 Roma ITALY

L.Davoli

Dipartimento di Matematica e Fisica, Universita' di Camerino

62032 Camerino ITALY

ABSTRACT

By comparison between the Mn K-edge x-ray absorption spectra of $[MnO_4]^-$ and $[Mn(OH_2)_6]^{2+}$ complexes in aqueous solution an experimental determination of the energy extent of the multiple scattering (MS) regime is obtained that is substantially wider than expected. Theoretical calculations based on the MS formalism support this conclusion. We rigorously show that the MS series for the absorption coefficient in these two clusters is convergent for all energies above the Mn 1s-3d transition. Based on this result a method of analysis is suggested for absorption spectra, capable in principle of providing higher order distribution functions $G_n(r_i)$ ($n \geq 3$) (beside the pair correlation function $G_2(r)$ usually obtained by EXAFS studies) and suitably generalizable to other cases of interest.

*Permanent address: Department of Thermology, Zaragoza University, SPAIN

Interest in local structure determination beyond the pair distribution function has recently stimulated the growing of X-ray Absorption Near Edge Structure (XANES) studies, both from a theoretical and an experimental point of view [1,2]. The reason for this lies in the fact that the low energy side of an absorption spectrum is sensitive to the geometrical arrangement of the environment surrounding the absorbing atom, due to the generally strong scattering power of the atoms of the medium in this energy region, which favors multiple scattering (MS) processes (in principle, up to infinite order) [3,4]. At energies such that the atomic scattering power becomes substantially small (in a way to be qualified later) a single scattering (SS) regime takes place, where the modulation in the absorption coefficient (EXAFS) is substantially due to the interference effect of the outgoing photoelectron wave from the absorbing atom and the backscattered wave from each surrounding atom [5,6]. Hence this latter part of the spectrum provides information about the pair correlation function. By decreasing the photoelectron kinetic energy a gradual turn over occurs from the EXAFS SS regime to the XANES full MS (FMS) regime through a transition region where only low order MS paths are expected to be relevant [7,8]. This last intermediate MS (IMS) region has received attention in the literature mainly in connection with collinear atomic configuration where the focussing effect makes collinear MS processes strong enough that they give an appreciable contribution even in the EXAFS region [6-9]. For open structures, i.e. structures with no collinear configurations, it has been suggested that "the transition region terminates with the XANES region itself" [10]. More recently an interpretation of Cu K-edge in terms of SS EXAFS theory with curved waves [11] and a Fourier analysis of the XANES region of $KMnO_4$ [12] have suggested that in these systems the MS energy range is very small and have questioned the capability of XANES to probe high order correlations.

It is the aim of this paper to critically assess the validity of these conclusions by presenting a unifying scheme of interpretation of x-ray absorption spectra based on a precise mathematical approach and corroborated by experimental evidence. To this purpose we have measured the K-edge absorption spectra of 50 mM of $MnCl_2$ and $KMnO_4$ aqueous solutions with high resolution. Mn ion in solution is octahedrally coordinated by 6 H_2O molecules forming a stable $[Mn(OH_2)_6]^{2+}$ cluster with a Mn-O distance $d_1 = 2.17 \text{ \AA}$ [13]. The tetrahedral cluster $[MnO_4]^-$ is known instead to be quite stable in

solution and its EXAFS has been analyzed by Rabe et al. [14] to give a Mn-O distance $d_2=1.63 \text{ \AA}$. Only the contribution of the first shell is present for photoelectron wave vector k above 5 \AA^{-1} in agreement with previous studies. In Fig. 1 the absorption spectra of $[\text{Mn}(\text{OH}_2)_6]^{2+}$ and $[\text{MnO}_4]^-$ are compared. The corresponding energy scales are in the ratio $(\frac{d_2^*}{d_1^*})^2 = 0.47$ where d_2^* and d_1^* are the Mn-O distances in the two complexes,

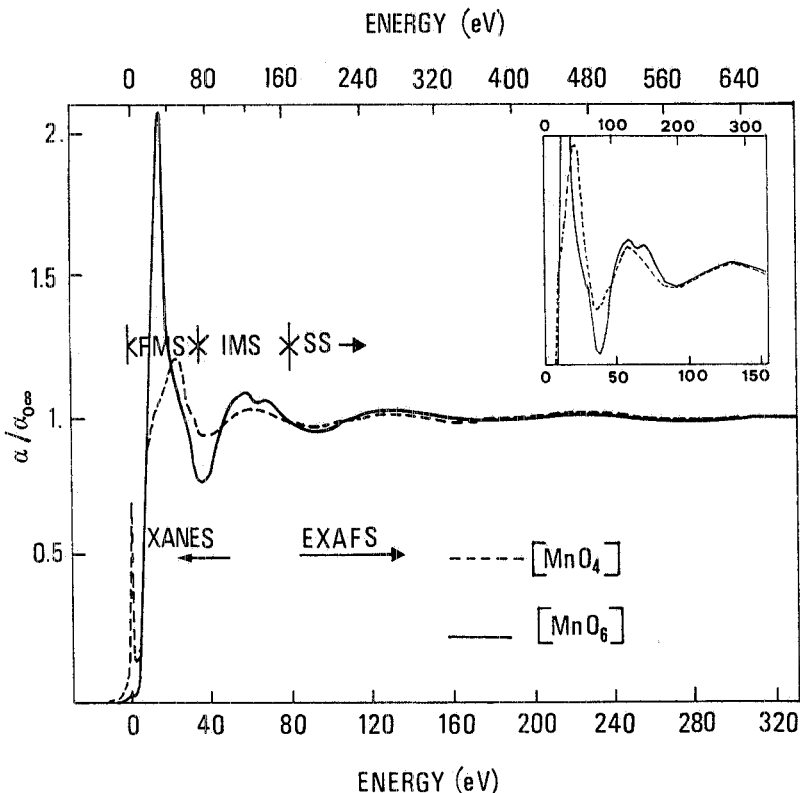


FIG. 1 - Comparison between normalized Mn K-edge X-ray absorption spectra of $[\text{MnO}_4]^-$ and $[\text{Mn}(\text{OH}_2)_6]^{2+}$ ions from 50 mM aqueous solution of K MnO_4 and MnCl_2 . The respective energy scales are given in the upper (lower) part of the figure. A partition of the spectra in FMS (full m.s.), IMS (Intermediate m.s.) and S.S (single scattering) regions is sketched. The insert shows a comparison of the two spectra after a rescaling of the oscillating amplitudes in the ratio 4:6.

corrected for the linear term coefficient of the scattering phase shift, in order to eliminate the effects in the spectra arising from the different bond length and from the dependence of the phase shifts on the energy. The zero of the energy has been set at the first absorption feature (1s-3d transition) in both spectra. In this way the two spectra, after a further rescaling of the oscillating amplitude to take into account the different number of nearest neighbors (see insert in Fig.1), show a superposed sinusoidal behavior in that energy region

that contains information only about the pair correlation function (EXAFS). Below 160 eV (75 eV with reference to $[Mn(OH_2)_6]^{2+}$ scale) the absorption spectrum of $[MnO_4]^-$ cluster deviates from the spectrum of $[Mn(OH_2)_6]^{2+}$. This fact is a clear indication that below these energies information about higher order correlation functions or geometrical arrangement of the environment of the absorbing atom is contained in the spectra.

In order to get a deeper insight into the MS region we have analyzed the spectra in the framework of MS concepts. In this formalism the polarization averaged absorption coefficient is given by [6,11,15]

$$\alpha_F = \alpha_F^{l+1} + \alpha_F^{l-1} = A \hbar \omega N_0 [(l+1)M_{l,l+1}^2 \chi_{l+1} + l M_{l,l-1}^2 \chi_{l-1}] \quad (1)$$

where l indicates the angular momentum of the core initial state ($l = 0$ for K-excitation) $M_{l,l\pm 1}^2$ is the atomic dipole transition matrix element relative to the photoabsorbing atom and

$$\chi_l = \frac{1}{2l+1} Im \chi_u = \frac{1}{2l+1} \frac{1}{sin^2 \delta_l^0} \sum_m Im[(I + T_a H)^{-1} T_a]_{lm,lm}^0 \quad (2)$$

where δ_l^0 is the phase shift of the absorbing atom located at site 0, I is the unit matrix, $H \equiv H_{LL}^i (1 - \delta_{ij})$ is the free amplitude of propagation of the photoelectron in a spherical wave state from site i with angular momentum $L \equiv (l, m)$ to site j with angular momentum $L' \equiv (l', m')$, $T_a \equiv (T_a)_{LL'}^j = \delta_{ij} \delta_{LL'} t_l^i$ is the diagonal matrix describing the scattering processes of the spherical wave with angular momentum l by the atom located at site i through the atomic t-matrix element $t_l^i = \exp(i\delta_l^i) \sin \delta_l^i$ and $T_a H$ implies matrix multiplication.

As apparent from eqn.(2) the whole geometrical information of the medium around the photoabsorber is contained in the matrix inverse $(I + T_a H)^{-1}$. In XANES calculation the full MS result eqn.(2) is compared with experimental data. However an alternative approach is viable, provided the condition $\rho(T_a H) < 1$ is verified for all relevant energies ($\rho(A)$ is the maximum eigenvalue of the matrix A). In such an instance $(I + T_a H)^{-1} = \sum_{n=0}^{\infty} (-1)^n (T_a H)^n$ where the series on the right is absolutely convergent relative to some matrix norm. Specializing to K-shell excitations (but the generalization is straightforward) we then have $\alpha_F = \sum_{n=0}^{\infty} \alpha_n$ where $\alpha_0 = A \hbar \omega N_0 M_{01}^2$ is the atomic absorption coefficient and

$$\alpha_n = \frac{\alpha_0}{3} \operatorname{Im} \chi_{11}^n = \frac{\alpha_0}{3} \frac{1}{\sin^2 \delta_1^0} (-1)^n \sum_m \operatorname{Im} [(T_a H)^n T_a]_{1m,1m}^0 \quad (3)$$

represents the partial contribution of order n to the absorption coefficient coming from all the processes where the photoelectron has been scattered $n-1$ times by the surrounding atoms before returning to the absorbing atom at site 0. Clearly α_n contains information about the n -th order correlation function. Notice that α_2 is the usual EXAFS signal times α_0 , whereas α_1 is always zero since $H_{1m,1m}^{0,0} = 0$. For the two clusters under consideration we have indeed found that the condition $\rho(T_a H) < 1$ is verified for all energies greater than a lower bound E_m , which is located just below the rising absorption jump edge. Hence an analysis of the experimental spectra in terms of the quantities α_n is meaningful. In Fig.2, we show a comparison between the calculated and experimental spectrum for $[Mn(OH_2)_6]^{2+}$ cluster for energies up to 140 eV. The calculation has been done using a multiple scattering program modified so that the inversion of the MS matrix $(I + T_a H)$ could be performed either exactly or through the series expansion, so that it was possible to construct explicitly the quantities α_n in eqn.(3). The $X - \alpha$ potential used was obtained through the usual Mattheis prescription. Hydrogen atoms were neglected. The agreement with experimental data is surprisingly good with respect to the shape of the spectrum. It is less good concerning the location of the high energy maxima due to the energy independence of the $X - \alpha$ potential used. In insert a) of Fig.2 the quantity α_F^c is the calculated absorption coefficient obtained by exact inversion of the MS matrix. The superscript c indicates convolution by an energy dependent Lorentian broadening function with $\Gamma_{tot}(E) = \Gamma_n + \Gamma_{exp} + \Gamma_{el}(E)$, where $\Gamma_n \approx 0.5$ eV is the core hole width, $\Gamma_{exp} \approx 1$ eV is the experimental resolution and $\Gamma_{el}(E)$ (of the order of 2 eV) is an energy dependent damping for the electron in the final state, taken from the imaginary part of the complex H.L. potential [16]. The experimental energy scale has been contracted by a factor 0.9 to correct for the energy independence of the $X - \alpha$ potential used [17]. Inserts b) and c) show the breakdown of α_F in terms of the partial contributions α_n for n up to 4. Apart from minor deviations, the sum $\alpha_0 + \alpha_2$ is already a good approximation to α_F for energies greater than 40 eV. So it would seem that EXAFS regime starts at this point. The agreement is however deceiving and is due to a fortuitous cancellation of the α_3 and α_4 contributions which are quite sizable and comparable in magnitude with α_2 in the whole energy range considered, but opposite in phase with each other (insert c). This

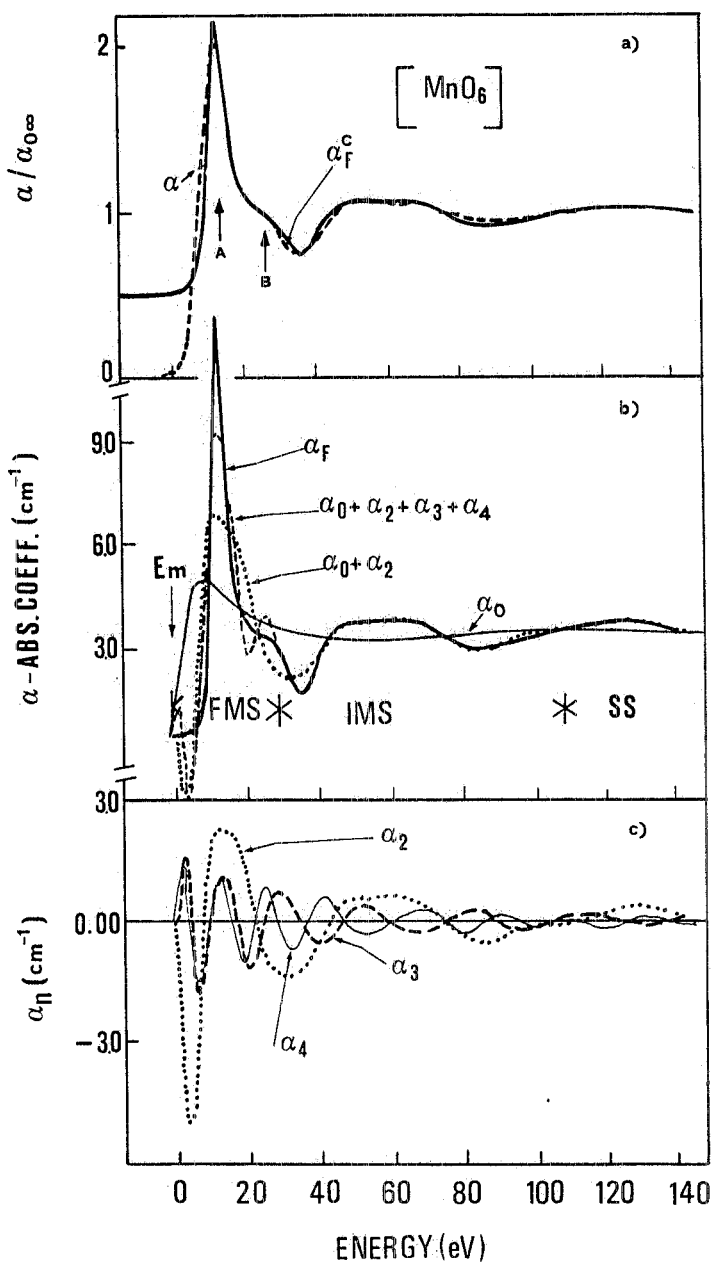


FIG. 2 - a) Comparison between experimental (α) and calculated (α_F^c) spectra for $[\text{Mn}(\text{OH}_2)_6]^{2+}$ cluster. The experimental energy scale has been contracted by a factor 0.9. The calculated curve has been convoluted with an energy dependent Lorentzian broadening function.
 b) Breakdown of the calculated bare spectrum α_F into the partial contributions $\sum_{n=0}^N \alpha_n$, for $N=0,2,4$. E_m indicates the lowest energy bound for the MS expansion to be valid. To obtain cross sections in Mb divide by 30.1.
 c) MS contributions of the n-th order to the absorption coefficient.

fact is due both to geometry (collinear configurations for paths of order higher than three) and to the particular value of the $l = 1$ phase shift of the absorbing atom ($\approx \pi$). At lower energies ($0 \div 40$ eV) contributions of MS paths coming from α_3 and α_4 are evident for feature B and feature A. In particular peak A gets contributions from all MS processes which, due to the particular geometrical coordination, happen to be all in phase at one particular energy (resonance energy). In this sense peak A is a resonance feature.

Fig.3 shows the same comparison for $[MnO_4]^{--}$ cluster. In this case the sum $\alpha_0 + \alpha_2 + \alpha_3$ is enough to get good agreement with α_F in the range $50 \div 140$ eV and in this interval α_n ($n \geq 4$) is negligible. Below 50 eV MS contributions of order higher than 3 are essential to get spectral features A and B. As before, feature B can be considered a broad resonance. The breakdown approach in terms of partial contributions to the absorption coefficient shows the continuous merging of the MS regime into the SS regime. However the merging interval is much larger than previously suspected. It ranges from 50 to 150 eV in $[MnO_4]^{--}$. Due to the convergence of the MS series, the higher the energy, the lower is the order of the correlation functions probed by the photoelectron. Damping considerations also corroborate this conclusion since damping increases the rate of convergence. In the two clusters under consideration its introduction does not alter substantially the above conclusions.

The general picture of an absorption spectrum that emerges from the preceding considerations consists a FMS region where many or an infinite number of MS paths of high order contribute to the final shape of the spectrum (sometimes the series does not converge at all), followed by an IMS region where only few MS paths of low order are relevant (typically $n \leq 4$), this region merging continuously into the EXAFS regime (SS region). The energy extent of each region is obviously system dependent.

Now the Fourier transform method that has been used successfully up to now to analyze EXAFS data does not seem to be suitable to sort out the MS contributions to the absorption coefficient. These contributions are either too small, so that peaks in configuration space due to MS paths are lost in the truncation ripples inherent in the Fourier transform of a limited K -range, or they give rise to too many peaks that merge into one broad feature of difficult interpretation. An alternative approach is suggested by the convergence of the series $\sum_{n=0}^{\infty} \alpha_n$ and by the fact that in the IMS region only low

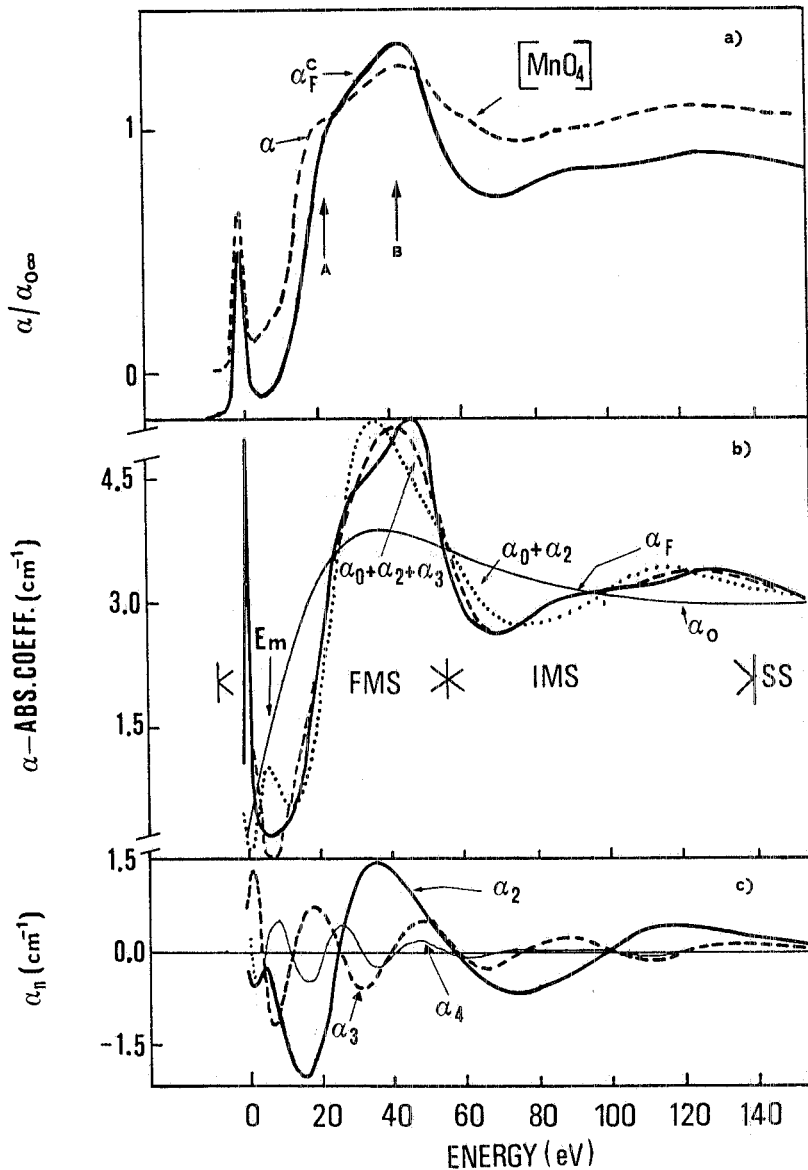


FIG. 3 - Same as Fig. 2, for $[\text{MnO}_4]^-$ cluster.

order paths ($n \leq 4$) are relevant. By generalizing a fitting procedure already used for EXAFS analysis [18], one can try to fit the entire absorption spectrum beyond the FMS region by the sum $\sum_{n=0}^4 \alpha_n$. This procedure might be carried out in successive steps, by first fitting the higher energy side by $\alpha_0 + \alpha_2$, to derive the atomic distances from the central atom. By adding α_3 one can try to fit a wider energy range to get a first guess to cross distances among surrounding atoms. Such guess could then be improved by adding α_4 to fit the entire region. Additional cross checks on the so derived geometrical structure

can than be obtained by fitting the FMS region using the exact expression eqn.(2). The necessary atomic phase shifts might be obtained from model compounds by applying the same procedure assuming the geometrical structure and using theoretical guesses based on a complex H.L. potential [16]. Mean free path considerations may be used to limit the size of the model cluster. Use of curved wave propagators is essential.

Since many-body effects are not accounted for by the present approach, except in a averaged way (use of complex potential), they should be dealt with separately. Summarizing we conclude that by careful analysis MS contributions to the absorption coefficient can be detected and utilized in energy regions of the spectrum which at a more superficial level of accuracy would be describable in terms of a SS theory only. The present experimental work has been performed at the Frascati Syncrotron Radiation Facility, run under joint CNR and INFN agreement.

References

- 1) A.Bianconi,L.Incoccia,S.Stipchich eds."Exafs and Near Edge Structure" Springer Series in Chem. Phys. vol 27 (1983)
- 2) F.W.Kutzler,C.R.Natoli,D.K.Misemer,S.Doniach,K.O.Hodgson J. Chem. Phys 73, 3274 (1980)
- 3) P.J.Durham,J.B.Pendry and C.H.Hodges, Solid State Comm. 38, 159 (1981)
- 4) A.Bianconi,M.Dell'Ariccia,P.J.Durham and J.B.Pendry Phys. Rev. B26, 6502 (1982)
- 5) D.E.Sayers,E.A.Stern and F.W.Lytte, Phys. Rev. Lett. 27, 1204 (1971)
- 6) P.A.Lee and J.B.Pendry, Phys.Rev B11, 2795 (1975)
- 7) C.R.Natoli, "Exafs and Near Edge Structure" Springer Series in Chem. Phys. vol 27, 43 (1983)
- 8) A.Bianconi, "Exafs and Near Edge Structure III" Springer Proc. Phys. vol 2, 167 (1984)
- 9) B.K.Teo, "Exafs and Near Edge Structure" Springer Series in Chem. Phys. vol 27 (1983)
- 10) J.B.Pendry, "Exafs and Near Edge Structure" Springer Series in Chem. Phys. vol 27 (1983)
- 11) J.E.Muller and W.L.Schaich, Phys. Rev. B27, 6489 (1983)
- 12) G.Bunker and E.A.Stern, Phys. Rev. Lett. 52, 1990 (1984)
- 13) G.Licheri and G.Pinna, Springer Series in Chemical Physics 27, 240 (1983)
- 14) P.Rabe,G.Tolkiehn and A.Werner, J. Phys.C 12, 1173 (1979)
- 15) P.J.Durham,J.B.Pendry and C.H.Hodges, Comp. Phys. Comm. 25, 193 (1982)
- 16) L.Hedin and B.I.Lundquist, J.Phys.C 4, 2064 (1971)
- 17) J.E.Muller,O.Jepsen and J.W.Wilkins, Solid State Comm. 42, 365 (1982)
- 18) N.Binsted,G.N.Greaves and C.M.B.Henderson Contrib. Mineral. Petrol. 89, 103 (1985)